Geochemical Journal, Vol. 47, pp. 459 to 468, 2013

In situ rutile U–Pb dating by laser ablation-MC-ICPMS

XIAOPING XIA,[1] ZHONGYUAN REN,[1] GANGJIAN WEI,[1]* LE ZHANG,[1] MIN SUN[2] and YUEJUN WANG[1]

[1]State Key Laboratory of Isotope Geochemistry, Guangzhou Institute of Geochemistry, Chinese Academy of Sciences, Guangzhou 510640, China
[2]Department of Earth Science, The University of Hong Kong, Pokfulam Road, Hong Kong, China

(*Received January 18, 2013; Accepted June 18, 2013*)

A method for *in situ* rutile U–Pb dating was developed using a multiple-collector (MC) ICPMS coupled to an excimer laser-ablation system. Compared with single collector Quadruple ICPMS used by previous *in situ* rutile U–Pb dating studies, the Neptune Plus MC-ICPMS used in this study has higher sensitivity and is capable of simultaneous acquisition of all the isotope signals required for rutile U–Pb dating. These advantages are important to achieve precise and reproducible *in situ* U–Pb dating results for rutiles, which typically contain low abundances of U and radiogenic Pb. The analytical results in this study on three reference rutile standards (R10, JDX and DXK) and one nature rutile sample (07RU3) agree with literature/known values, thereby demonstrating that this technique can yield precise and accurate U–Pb dating results for Paleozoic to Paleoproterozoic rutile, even with ~1 ppm U.

Keywords: laser ablation, MC-ICPMS, rutile, U–Pb dating, *in situ*

INTRODUCTION

Laser ablation combined with inductively coupled plasma mass spectrometry (LA-ICP-MS) has been widely used in geochronological research in the last two decades. The LA-ICP-MS method has been widely applied to U–Pb zircon dating, which can yield analytical precision comparable to that of the secondary ion microprobe (SIMS) technique (Horn *et al*., 2000; Simonetti *et al*., 2008; Xia *et al*., 2004). Rutile (TiO_2) is a common accessory mineral, which is common in many igneous, metamorphic and sedimentary rocks. It is stable over a wide range of *P–T* conditions and is resistant to weathering, transportation and diagenesis (Morton and Hallsworth, 1994) and hosts measureable U and radiogenic Pb. Previous studies have demonstrated that rutile can be used as a precise geochronometer and in particular has important applications for metamorphic rocks (Kylander-Clark *et al*., 2008; Li *et al*., 2011). Traditional isotope dilution-TIMS method has been applied to several U–Pb rutile dating studies, although it often suffers from mineral inclusions and retrograde rims of titanite with high proportions of common lead (Xiao *et al*., 2006). Single collector LA-ICPMS has been employed for *in situ* U–Pb rutile dating in pioneering works by Storey *et al*. (2007), Birch *et al*. (2007), Zack *et al*. (2011) and Kooijman *et al*. (2010). This method is limited to rutile grains with sufficient U in order to get suitable Pb signal intensity (Zack *et al*., 2011). It is well known that multi collector ICPMS offers advantages in terms of higher sensitivity, flat top peak shape and simultaneous acquisition, features ideal for precise isotope ratio analyses. Some researchers have applied LA-MC-ICPMS to U–Pb rutile dating such as Vry and Baker (2006), Warren *et al*. (2012) and Bracciali *et al*. (2013), but the amount of works using this method are limited, and Vry and Baker (2006) only obtained Pb–Pb ages and no U–Pb ages. Therefore the potential of LA-MC-ICPMS to rutile U–Pb dating has not been fully explored. We hereby report a new analytical protocol and the analytical results for 4 different natural rutile samples using LA-MC-ICPMS in this paper. Our results demonstrate that this technique can yield precise and accurate U–Pb dating results for rutile even with *ca*. 1 ppm U.

*Corresponding author (e-mail: gjwei@gig.ac.cn)

ANALYTICAL METHOD

Instrumentation

A Neptune Plus multi collector ICP-MS installed at the State Key Laboratory of Isotope Geochemistry, Guangzhou Institute of Geochemistry, Chinese Academy of Sciences (GIGCAS) was employed in this study. The MC-ICPMS is fitted with a collector block containing 9 variable position Faraday cups and 8 Ion Counters (compact discrete dynamic multiplier, CDD or SEM). This collector system has a relative mass range of more than

Table 1. Operating conditions and instrument parameters

Laboratory and Sample Preparation	
Laboratory name	State Key Laboratory of Isotope Geochemistry, Guangzhou
Sample type/mineral	Rutile
Sample preparation	Conventional mineral separation, 1 inch resin mount
Laser Ablation System	
Make, model and type	Resonetics LLC USA, RESOlution M-50, ArF excimer
Ablation cell and volume	Two-volume laser-ablation cell (Laurin Technic, Australia), effective volume ~1–2 cm^3
Laser wavelength	193 nm
Pulse width	~20 ns
Fluence	4 $J \cdot cm^{-2}$
Repetition rate	5 Hz
Spot size	44 um
Sampling mode/pattern	Spot
Carrier gas	700 ml/min He + 2 ml/min N_2, Ar make-up gas
Ablation duration	30 seconds
ICP-MS Instrument	
Make, model and type	Thernmo Fisher Scientific, Neptune Plus, MC-ICP-MS
Sample introduction	Ablation aerosol
RF power	1200 W
Make-up gas flow	400 ml/min Ar
Detection system	Mixed Faraday-multiple ion counting array
Masses measured	202, 204, 206, 207, 208, 232 238
Data Processing	
Gas blank	30 seconds on-peak zero subtracted
Calibration strategy	R19 rutile standard used as primary reference material
Reference Material info	R19 $^{206}Pb/^{238}U$ 489.5 ± 0.9 Ma, $^{207}Pb/^{206}Pb$ 489.8 ± 9.3Ma (Zack *et al*., 2011)
Data processing package used	In-house created spreadsheet program
Uncertainty level and propagation	Ages are quoted at 2 sigma absolute, propagation is by quadratic addition. Reproducibility and age uncertainty of reference material are propagated.
Other information	Sample line of 2.5 m from ablation cell to torch and a 30 seconds washout time after the laser stopped firing

17%, allowing simultaneous acquisition of ion signals ranging from mass ^{202}Hg to ^{238}U, an important factor in obtaining highly precise and accurate U–Pb age determinations. With a 100 μL/min PFA standard concentric nebulizer, dual-pass spray chamber, standard sample cone and H-skimmer cone, this instrument commonly gives a sensitivity of >1200 V for 1 ppm solution of ^{238}U. The ICP-MS was equipped with an ArF excimer 193 nm RESOlution M-50 (Resonetics LLC, USA), which has been described in detail by Müller *et al*. (2009). This system can wash out 99% of the signal in less than 1.5 seconds due to its innovative sample cell design. Helium gas, which carries the laser-ablated sample aerosol from the sample cell, is mixed with argon carrier gas along with nitrogen as an additional di-atomic gas to enhance sensitivity, and finally flows into the MC-ICPMS torch. The operating conditions for this study are summarized in Table 1.

Analytical protocols

Samples were prepared as grain mounts. The mounts were well polished to expose the fresh interior of the crystals. Thorough cleaning were made by polishing the surface with alumina powder and then putting in an ultrasonic bath for 5 minutes with milli-Q water and finally drying with ethanol-soaked kimwipe paper.

Prior to analysis, gas flow rates of argon make-up gas, helium and nitrogen carrier gas were optimized to achieve maximum sensitivity with low oxide production ($^{254}UO/^{238}U < 1\%$). Laser settings used for sample analyses include a beam diameter of *ca*. 44 μm, 5 Hz repetition rate, and energy intensity on target of about 4.0 J. The rutile was pre-ablated by five laser pulses before analysis in order to remove the surface common-lead contamination. Each analysis incorporated a background acquisition of approximately 30 seconds (gas blank, closing the laser shutter) followed by 30 seconds of data acquisition for the sample, which usually leave ablated pits with depth of ~20 μm. ^{208}Pb, ^{207}Pb, ^{206}Pb, ^{204}Pb (+^{204}Hg) and ^{202}Hg signals were measured on the ion counters, whereas ^{238}U and ^{232}Th were acquired on the Faraday cups. In order to check the linearity of the ion counters, the rutile R10 (see below) is ablated with variable laser fluences, spot size or repetition rate so as to achieve ^{206}Pb signal from <50000

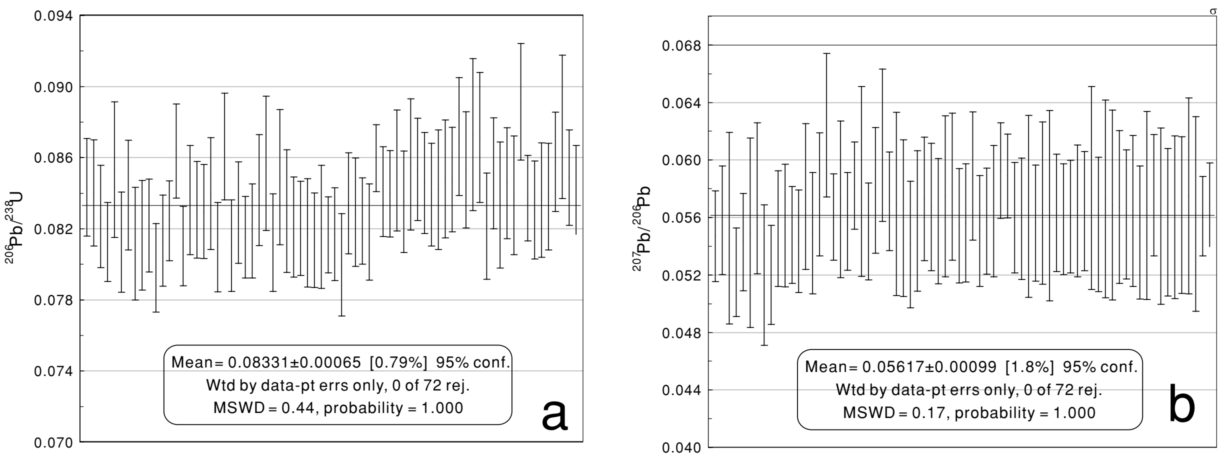

Fig. 1. Measured raw ratios of $^{206}Pb/^{238}U$ (a) and $^{207}Pb/^{206}Pb$ (b) for external calibration standard rutile R19. Data-point error bars are 1σ.

to >1000000 counts per second. Consistent common lead corrected $^{207}Pb/^{206}Pb$ ratios with external precision of <0.3% demonstrated a good linearity of the ion counters.

Corrections for instrumental drift, mass bias and $^{206}Pb/^{238}U$ fractionation were all conducted by a "standard-sample-standard" bracketing external standardization technique. One piece of standard rutile R19 with a size of ~2 × 1 × 2 mm was used for this purpose. The crystal from which it is derived is a *ca*. 500 mm^3 sized single crystal from Blumberg, Australia. Detailed trace elements, Hf isotope and U–Pb age studies have been conducted for this standard (Luvizotto *et al*., 2009; Zack *et al*., 2011). A weighted mean $^{206}Pb/^{238}U$ age of 489.5 ± 0.9 Ma obtained by the TIMS method (Zack *et al*., 2011) was adopted as the reference material in this study. It was analyzed three times every five analyses of unknown. A multi-collector ICPMS cannot measure an internal element standard if it requires a large mass jump such as needed for ^{49}Ti, and so accurate U and Pb concentrations were impossible to obtain. However, in order to characterize the analyzed piece of rutile, approximate U concentration data were obtained by direct comparing the signal intensities between the unknown and external standard NIST SRM 610 assuming they have the same signal yield for the same analytical conditions. NIST SRM 610 was analyzed twice every five analyses of unknown. The U concentration value of NIST SRM 610 used for external calibration was taken from Pearce *et al*. (1997).

Off-line data reduction (including selection and integration of background and analyte signals) was performed by a spreadsheet program created by the authors. The time-resolved signal of single isotopes and isotope ratios was carefully inspected to verify the presence of perturbations related to inclusions, fractures and mixing of different age domains. The mean ratios of $^{232}Th/^{238}U$, $^{206}Pb/^{208}Pb$, $^{207}Pb/^{206}Pb$ and $^{206}Pb/^{238}U$ were calculated directly based on the background subtracted raw signals. No $^{206}Pb/^{238}U$ fractionation is corrected for individual analyses besides the external standardization. The analytical uncertainties of the ratios were calculated based on standard deviation divided by square root of (n–1), n being the number of the time-resolved isotope ratios. Common-lead correction was performed by estimating the common-lead content based on the ^{208}Pb signal intensity assuming all the ^{208}Pb measured is non-radiogenic, as rutiles contain extremely low content of Th (Zack *et al*., 2011). A two-stage Pb evolution model of Stacey and Kramers (1975) was adopted. Time-dependent machine drift, mass bias and elemental fractionation were all corrected using a linear interpolation (with time) for every five analyses, according to the variations of the standard rutile R19.

In this study a dataset of 72 spot analyses were collected during about 6 hours for the external standard R19, which gave a reproducibility of 0.79% (95% confidence, MSWD = 0.44) for $^{207}Pb/^{206}Pb$ and 1.8% (95% confidence, MSWD = 0.17) for $^{206}Pb/^{238}U$ (Fig. 1). This uncertainty was propagated for each individual sample analysis following Horstwood *et al*. (2003). Therefore the ratio/age error quoted in the Table 2 comes from two sources: uncertainty of individual (single spot) analyses mainly due to counting statistics of the signals, and external standardization. The $^{207}Pb/^{235}U$ ratio is derived from the normalized and error propagated $^{207}Pb/^{206}Pb$ and $^{206}Pb/^{238}U$ ratios assuming a $^{238}U/^{235}U$ natural abundance ratio of 137.88, and the uncertainty is derived from the quadratic addition of the propagated uncertainties of both ratios. Concordia diagrams and weighted mean calculations were made using Isoplot V3.

Table 2. Rutile U–Pb analyzed by LA-MCICPMS

Sample No.	U concentration	Corrected ratios							Error correlations*	Ages						
		Th/U	$^{206}Pb/^{208}Pb$	$^{207}Pb/^{206}Pb$	1σ [%]	$^{207}Pb/^{235}U$	1σ [%]	$^{206}Pb/^{238}U$	1σ [%]	$^{207}Pb/^{206}Pb$	$2\sigma_{abs}$	$^{207}Pb/^{235}U$	$2\sigma_{abs}$	$^{206}Pb/^{238}U$	$2\sigma_{abs}$	Concordance** [%]
Rutile R10																
R10-1	45	0.0005	324	0.076	2.3	1.93	3.4	0.184	2.5	0.7	1099	45	1092	22	1088	25	100
R10-2	45	0.0009	302	0.076	2.3	1.88	2.9	0.180	1.8	0.6	1083	46	1073	19	1068	18	100
R10-3	45	0.0005	1158	0.076	3.3	1.96	3.8	0.187	1.9	0.5	1089	64	1100	25	1106	19	99
R10-4	43	0.0004	408	0.076	2.4	1.97	3.0	0.189	1.8	0.6	1089	47	1106	20	1115	18	99
R10-5	44	0.0005	63	0.075	2.8	1.90	4.3	0.183	3.3	0.8	1077	56	1080	28	1082	32	100
R10-6	42	0.0001	72	0.076	2.7	1.90	3.9	0.183	2.7	0.7	1082	53	1083	25	1083	27	100
R10-7	44	0.0001	73	0.075	3.2	1.94	4.6	0.187	3.3	0.7	1074	62	1093	30	1103	34	99
R10-8	45	0.0002	60	0.075	2.8	1.91	3.4	0.185	2.0	0.6	1072	56	1086	23	1092	20	99
R10-9	44	0.0000	95	0.076	2.9	1.96	3.8	0.188	2.5	0.7	1086	56	1101	25	1109	26	99
R10-10	47	0.0006	436	0.076	2.4	1.91	4.0	0.183	3.2	0.8	1089	48	1086	26	1084	32	100
R10-11	53	0.0003	567	0.076	2.4	1.92	2.8	0.183	1.5	0.5	1091	48	1088	19	1086	15	100
R10-12	44	0.0006	154	0.076	2.6	1.92	3.8	0.183	2.8	0.7	1096	51	1087	25	1082	28	100
R10-13	41	0.0001	84	0.075	3.2	1.92	4.1	0.186	2.7	0.6	1070	62	1089	27	1099	27	99
R10-14	41	0.0009	108	0.076	2.3	1.90	4.2	0.181	3.6	0.8	1093	46	1080	28	1074	35	99
R10-15	41	0.0005	89	0.076	2.5	1.91	3.6	0.183	2.6	0.7	1082	49	1084	24	1085	25	100
R10-16	42	0.0001	235	0.076	2.3	1.92	4.0	0.184	3.3	0.8	1092	46	1090	27	1089	33	100
R10-17	36	0.0003	1181	0.076	2.5	1.94	4.3	0.186	3.5	0.8	1093	49	1096	29	1098	36	100
R10-18	40	0.0007	106	0.075	3.3	1.92	5.0	0.185	3.7	0.7	1078	65	1089	33	1095	38	99
R10-19	45	0.0001	489	0.076	2.5	1.94	3.9	0.185	3.0	0.8	1100	49	1097	26	1095	30	100
R10-20	41	0.0000	22	0.076	3.9	1.98	4.9	0.189	3.0	0.6	1091	77	1108	33	1116	31	99
R10-21	35	0.0000	68	0.075	3.1	1.96	4.7	0.188	3.5	0.7	1081	61	1102	31	1112	36	99
R10-22	42	0.0000	2833	0.076	3.1	1.89	4.9	0.181	3.7	0.8	1091	61	1079	32	1073	37	99
R10-23	35	0.0001	42	0.075	2.9	1.96	4.5	0.189	3.5	0.8	1072	57	1101	30	1116	35	99
										Aver.	1085.7		1090.9		1093.5		
Rutile DXK																	
DXK-1	8	0.0009	639	0.110	2.5	4.87	5.2	0.322	4.6	0.9	1793	45	1798	43	1802	72	100
DXK-2	8	0.0112	380	0.109	2.7	4.77	5.8	0.316	5.1	0.9	1787	48	1779	47	1773	78	100
DXK-3	8	0.0063	114	0.110	3.2	4.75	5.5	0.314	4.4	0.8	1793	58	1776	45	1761	68	99
DXK-4	7	0.0001	266	0.109	3.7	4.77	7.2	0.316	6.1	0.9	1788	65	1779	58	1771	94	100
DXK-5	8	0.0011	200	0.110	3.9	4.73	6.6	0.312	5.3	0.8	1797	69	1773	54	1752	81	99
DXK-6	8	0.0014	187	0.110	3.4	4.69	5.7	0.309	4.6	0.8	1799	61	1765	47	1736	69	98
DXK-7	9	0.0097	138	0.109	3.2	4.78	6.2	0.319	5.3	0.9	1777	57	1781	51	1784	82	100
DXK-8	9	0.0073	200	0.109	3.4	4.80	6.2	0.318	5.3	0.8	1786	60	1784	51	1782	81	100
DXK-9	4	0.0098	93	0.110	4.0	4.81	6.7	0.317	5.4	0.8	1803	71	1787	55	1773	83	99
DXK-10	8	0.0036	447	0.110	3.0	4.84	5.4	0.320	4.6	0.8	1793	54	1792	45	1792	71	100
DXK-11	8	0.0104	113	0.108	4.2	4.81	6.4	0.322	4.8	0.8	1774	75	1787	52	1798	75	99
DXK-12	8	0.0155	113	0.108	3.9	4.73	6.5	0.319	5.2	0.8	1759	69	1773	53	1785	81	99
DXK-13	10	0.0228	74	0.108	3.5	4.67	6.2	0.315	5.1	0.8	1762	62	1763	51	1763	79	100
DXK-14	7	0.0051	364	0.109	2.6	4.85	5.3	0.323	4.6	0.9	1779	48	1793	44	1806	72	99
DXK-15	11	0.0365	51	0.107	2.4	4.73	6.0	0.320	5.5	0.9	1751	43	1772	49	1789	85	99

Sample No.	U concentration	Corrected ratios								Error correlations*	Ages						
		Th/U	$^{206}Pb/^{208}Pb$	$^{207}Pb/^{206}Pb$	1σ [%]	$^{207}Pb/^{235}U$	1σ [%]	$^{206}Pb/^{238}U$	1σ [%]		$^{207}Pb/^{206}Pb$	$2\sigma_{abs}$	$^{207}Pb/^{235}U$	$2\sigma_{abs}$	$^{206}Pb/^{238}U$	$2\sigma_{abs}$	Concordance** [%]
DXK-16	8	0.0012	532	0.110	2.6	4.84	5.8	0.320	5.2	0.9	1796	47	1792	48	1788	81	100
DXK-17	7	0.0072	224	0.110	3.2	4.83	5.7	0.320	4.7	0.8	1792	58	1790	47	1789	73	100
DXK-18	8	0.0065	290	0.109	2.6	4.84	5.3	0.323	4.6	0.9	1775	46	1792	44	1807	73	99
DXK-19	7	0.0053	875	0.110	2.7	4.89	4.8	0.324	4.0	0.8	1792	48	1801	40	1809	64	100
DXK-20	8	0.0018	295	0.109	2.7	4.87	5.1	0.325	4.4	0.9	1777	48	1798	42	1816	69	99
DXK-22	9	0.0215	89	0.107	3.0	4.60	5.3	0.312	4.4	0.8	1748	54	1749	44	1749	67	100
DXK-23	8	0.0132	171	0.108	3.3	4.68	5.5	0.314	4.4	0.8	1771	59	1764	45	1758	67	100
DXK-24	5	0.0107	110	0.109	3.4	4.80	5.8	0.319	4.7	0.8	1786	61	1785	47	1784	72	100
DXK-25	7	0.0102	503	0.109	2.8	4.79	4.8	0.318	3.9	0.8	1790	50	1784	40	1779	61	100
DXK-26	8	0.0002	402	0.109	3.0	4.68	5.9	0.312	5.1	0.9	1781	53	1763	48	1749	78	99
DXK-27	7	0.0078	159	0.110	3.0	4.75	5.0	0.312	4.0	0.8	1806	53	1775	41	1749	62	99
DXK-28	5	0.0055	282	0.110	3.6	4.74	5.7	0.313	4.4	0.8	1795	64	1775	47	1758	68	99
DXK-29	8	0.0043	133	0.108	2.7	4.84	6.0	0.324	5.4	0.9	1773	48	1793	49	1809	84	99
DXK-30	9	0.0151	191	0.108	2.7	4.79	5.6	0.321	5.0	0.9	1772	48	1784	46	1794	78	99
DXK-31	6	0.0001	5092	0.110	2.8	4.83	5.1	0.318	4.2	0.8	1802	49	1790	42	1781	66	99
DXK-32	6	0.0029	563	0.110	2.9	4.69	4.3	0.309	3.1	0.7	1801	52	1766	35	1737	47	98
DXK-33	6	0.0088	7	0.109	2.7	4.86	5.3	0.322	4.5	0.9	1789	49	1795	44	1800	71	100
DXK-34	9	0.0070	202	0.108	2.6	4.75	4.7	0.318	4.0	0.8	1774	47	1777	39	1779	61	100
DXK-35	9	0.0047	12	0.109	3.4	4.76	5.3	0.318	4.0	0.8	1779	61	1779	43	1778	62	100
										Aver.	1783.5		1781.0		1778.8		
Rutile JDX																	
JDX-1	14	0.0020	214	0.058	6.8	0.66	7.9	0.082	3.9	0.5	523	143	513	31	511	19	100
JDX-2	14	0.0031	449	0.057	4.9	0.65	6.0	0.083	3.5	0.6	507	104	510	24	511	17	100
JDX-3	10	0.0033	143	0.058	5.7	0.66	7.3	0.083	4.6	0.6	512	120	515	29	515	23	100
JDX-4	12	0.0010	177	0.058	5.5	0.66	6.5	0.082	3.6	0.6	520	116	512	26	510	18	100
JDX-5	13	0.0022	2345	0.058	3.7	0.66	4.7	0.083	3.0	0.6	519	79	516	19	515	15	100
JDX-6	14	0.0012	407	0.058	5.0	0.66	5.7	0.084	2.8	0.5	516	106	517	23	517	14	100
JDX-7	11	0.0012	245	0.057	6.0	0.65	7.2	0.082	3.9	0.5	505	127	510	28	511	19	100
JDX-8	14	0.0029	85	0.058	5.8	0.66	6.9	0.082	3.7	0.5	535	122	514	27	509	18	99
JDX-9	14	0.0000	955	0.058	3.7	0.65	4.9	0.082	3.2	0.7	530	80	510	20	506	16	99
JDX-10	14	0.0003	332	0.058	4.5	0.65	5.4	0.082	3.1	0.6	535	95	511	22	505	15	99
JDX-11	15	0.0014	179	0.057	5.6	0.66	6.6	0.083	3.5	0.5	508	118	512	26	513	17	100
JDX-12	14	0.0025	148	0.058	5.5	0.66	6.7	0.082	3.9	0.6	525	115	512	27	509	19	99
JDX-13	8	0.0023	300	0.058	5.2	0.67	7.4	0.083	5.3	0.7	528	110	518	30	515	26	100
JDX-14	8	0.0016	285	0.057	5.0	0.64	6.2	0.081	3.7	0.6	505	106	502	24	501	18	100
JDX-15	9	0.0075	68	0.057	6.2	0.63	8.7	0.080	6.1	0.7	501	132	499	34	499	29	100
JDX-16	13	0.0020	237	0.058	4.0	0.65	5.6	0.082	4.0	0.7	513	85	509	22	508	19	100
JDX-17	13	0.0015	1998	0.058	3.8	0.65	5.0	0.081	3.3	0.7	515	81	506	20	504	16	100
JDX-18	13	0.0020	302	0.058	4.7	0.64	5.8	0.081	3.4	0.6	522	101	505	23	502	16	99
JDX-19	12	0.0045	287	0.058	4.8	0.64	6.1	0.081	3.7	0.6	515	102	505	24	503	18	100
JDX-20	12	0.0027	144	0.059	6.5	0.66	7.5	0.081	3.6	0.5	564	136	514	30	503	17	98

*Error correlation is calculated as $({}^{207}Pb/{}^{235}U_{error}{}^{2} + {}^{206}Pb/{}^{238}U^{2} - {}^{207}Pb/{}^{206}Pb_{error}{}^{2})/(2*{}^{207}Pb/{}^{235}U*{}^{206}Pb/{}^{238}U)$.
**Concordance is calculated as 100–100*abs($^{207}Pb/^{235}U$ age – $^{206}Pb/^{238}U$ age)/$^{206}Pb/^{238}U$ age.

Table 2. (continued)

Sample No.	U concentration	Corrected ratios								Error correlations*	Ages						
		Th/U	$^{206}Pb/^{208}Pb$	$^{207}Pb/^{206}Pb$	1σ [%]	$^{207}Pb/^{235}U$	1σ [%]	$^{206}Pb/^{238}U$	1σ [%]		$^{207}Pb/^{206}Pb$	$2\sigma_{abs}$	$^{207}Pb/^{235}U$	$2\sigma_{abs}$	$^{206}Pb/^{238}U$	$2\sigma_{abs}$	Concordance** [%]
JDX-21	12	0.0343	4	0.058	4.2	0.65	6.5	0.082	4.9	0.8	540	89	511	26	505	24	99
JDX-22	11	0.0026	224	0.057	6.4	0.65	7.4	0.082	3.7	0.5	503	134	508	29	510	18	100
JDX-23	12	0.0008	506	0.058	4.2	0.65	5.7	0.082	3.8	0.7	517	90	509	22	507	18	100
JDX-24	12	0.0022	186	0.058	7.2	0.64	7.9	0.081	3.4	0.4	514	150	503	31	500	16	99
JDX-25	12	0.0382	3	0.058	4.3	0.65	5.5	0.081	3.5	0.6	544	91	508	22	500	17	98
JDX-26	12	0.0001	350	0.058	5.2	0.66	6.1	0.083	3.2	0.5	517	111	515	24	514	16	100
JDX-27	13	0.0015	208	0.058	6.3	0.66	7.5	0.082	4.2	0.6	533	131	514	30	510	20	99
JDX-28	13	0.0024	2832	0.058	3.6	0.67	5.2	0.084	3.8	0.7	515	76	521	21	522	19	100
JDX-29	12	0.0016	3653	0.058	4.1	0.66	5.7	0.083	4.0	0.7	515	87	513	23	512	20	100
JDX-30	12	0.0011	210	0.058	6.3	0.66	7.4	0.083	3.8	0.5	532	133	516	29	513	19	99
JDX-31	12	0.0035	580	0.058	5.2	0.66	6.5	0.083	3.8	0.6	513	111	512	26	512	19	100
JDX-32	9	0.0000	3092	0.058	4.4	0.67	6.6	0.083	4.9	0.7	540	94	519	26	514	24	99
JDX-33	9	0.0000	–2314	0.058	4.8	0.67	7.1	0.084	5.3	0.7	521	101	522	29	522	27	100
JDX-34	8	0.0000	–2330	0.057	4.4	0.67	6.3	0.084	4.5	0.7	503	93	519	25	522	22	99
										Aver.	520.7		511.5		509.7		
Rutile 07RU3																	
07RU3-1	1.1	0.0000	17	0.053	17.9	0.38	18.4	0.052	4.2	0.2	309	364	325	50	327	13	99
07RU3-2	1.1	0.0000	6	0.053	20.6	0.38	22.1	0.052	8.0	0.4	343	409	327	60	324	25	99
07RU3-3	1.1	0.0000	18	0.053	15.8	0.37	16.3	0.051	4.0	0.2	313	324	322	44	323	13	100
07RU3-4	1.2	0.0001	25	0.055	17.8	0.40	18.4	0.053	4.6	0.3	428	355	343	52	330	15	96
07RU3-5	1.2	0.0000	3	0.052	17.1	0.37	18.7	0.051	7.4	0.4	266	352	317	50	324	23	98
07RU3-6	1.2	0.0001	14	0.051	17.3	0.37	17.7	0.052	3.8	0.2	224	357	316	47	329	12	96
07RU3-7	1.1	0.0000	24	0.051	21.3	0.35	21.7	0.051	4.2	0.2	219	431	307	56	319	13	96
07RU3-8	1.1	0.0000	12	0.053	17.5	0.37	18.0	0.051	4.4	0.2	309	356	317	48	318	14	100
07RU3-9	1.0	0.0011	1	0.052	14.3	0.36	15.2	0.051	5.0	0.3	290	298	315	40	318	15	99
07RU3-10	1.0	0.0011	1	0.052	14.3	0.37	15.2	0.051	5.0	0.3	299	298	319	41	321	16	99
07RU3-11	1.0	0.0034	2	0.049	15.5	0.35	16.0	0.052	3.7	0.2	147	329	307	41	329	12	93
07RU3-12	1.1	0.0002	72	0.050	16.9	0.37	17.4	0.053	4.0	0.2	193	351	317	46	334	13	95
07RU3-13	0.9	0.0000	18	0.052	16.8	0.37	17.3	0.052	4.1	0.2	268	346	322	47	329	13	98
07RU3-14	1.0	0.0000	11	0.048	16.9	0.35	17.4	0.052	4.0	0.2	122	356	304	45	328	13	93
07RU3-15	0.8	0.0044	1	0.052	12.5	0.36	12.9	0.050	3.3	0.3	277	263	313	34	317	10	98
07RU3-16	1.1	0.0004	10	0.056	17.5	0.40	18.0	0.052	4.1	0.2	437	348	339	50	325	13	96
07RU3-17	1.1	0.0001	7	0.052	18.2	0.36	19.0	0.051	5.3	0.3	284	370	315	50	319	16	99
07RU3-18	1.1	0.0002	5	0.050	12.9	0.37	13.6	0.053	4.3	0.3	213	274	317	36	331	14	96
07RU3-19	1.0	0.0006	2	0.052	18.1	0.38	18.6	0.053	4.2	0.2	300	368	327	51	331	14	99
07RU3-20	1.0	0.0025	1	0.055	13.4	0.39	14.0	0.051	4.1	0.3	418	274	333	39	321	13	96
07RU3-21	1.0	0.0000	25	0.049	18.9	0.35	19.4	0.052	4.1	0.2	127	394	304	50	328	13	93
07RU3-22	1.2	0.0000	14	0.047	21.3	0.34	21.8	0.052	4.9	0.2	69	441	297	55	326	16	91
07RU3-23	1.1	0.0000	14	0.050	17.9	0.36	18.4	0.052	4.2	0.2	206	370	310	48	324	13	96
07RU3-24	1.1	0.0000	40	0.054	18.1	0.39	18.5	0.053	3.4	0.2	366	364	335	51	330	11	99
										Aver.	267.8		318.7		325.2		

*Error correlation is calculated as $(^{207}Pb/^{235}U_{error}{}^2 + {}^{206}Pb/^{238}U^2 - {}^{207}Pb/^{206}Pb_{error}{}^2)/(2 * {}^{207}Pb/^{235}U * {}^{206}Pb/^{238}U)$.
**Concordance is calculated as 100–100*abs($^{207}Pb/^{235}U$ age – $^{206}Pb/^{238}U$ age)/$^{206}Pb/^{238}U$ age.

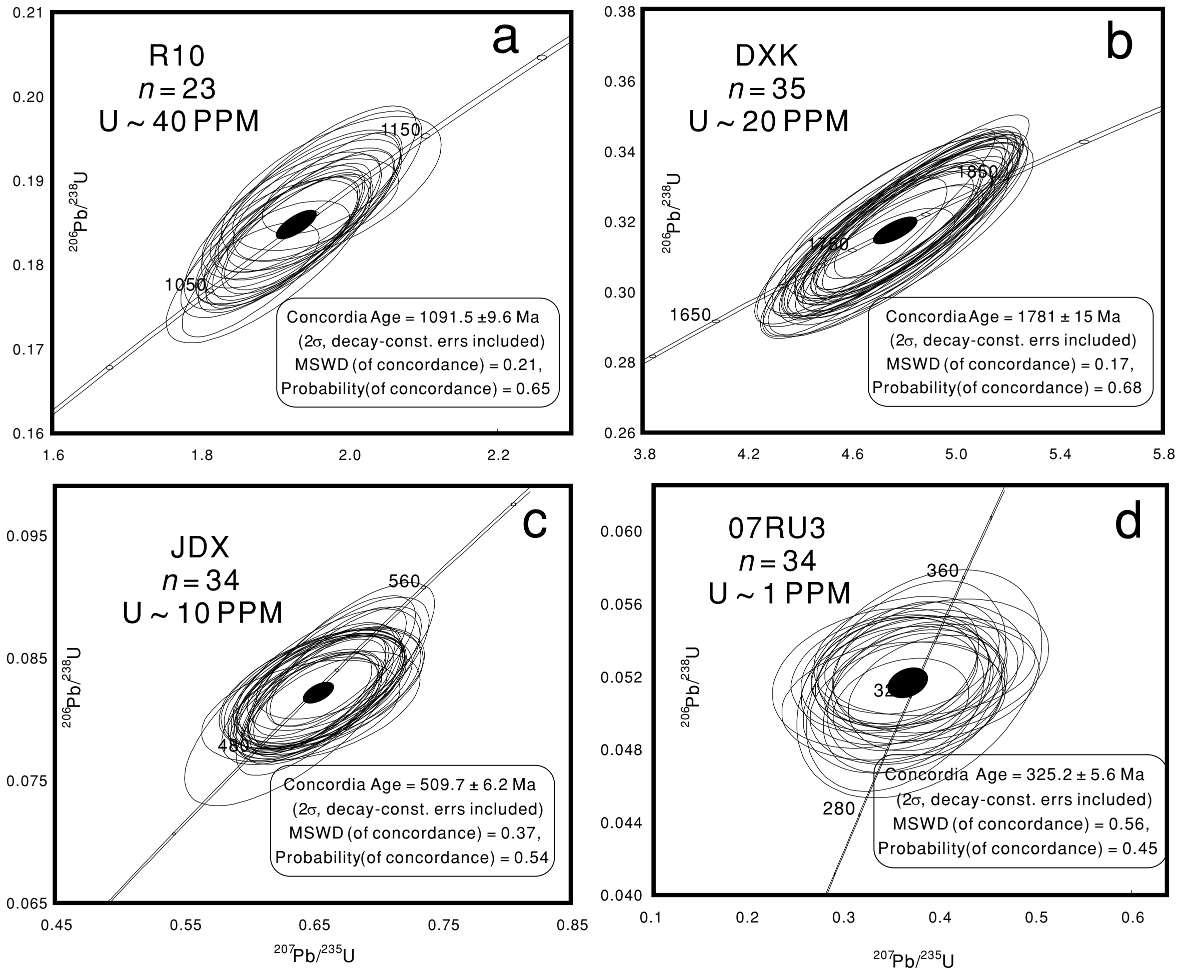

Fig. 2. U–Pb concordia diagrams showing the analytical results for standard rutiles R10 (a), DKX (b), JDX (c) and the unknown sample 07RU3 (d). Data-point error ellipses are 1σ. MSWD is the mean square of weighted deviations.

Results and Discussion

Secondary rutile standards used in this study are one international rutile standard (R10) (Luvizotto *et al*., 2009), two in-house rutile standards (JDX and DXK) (Li *et al*., 2011) and one unknown nature rutile sample 07RU3. The analytical results obtained in this study are listed in the Table 2.

Rutile standard R10

This rutile has been widely used in LA-ICPMS and SIMS labs for U–Pb isotope analyses (Kooijman *et al*., 2010; Li *et al*., 2011; Zack *et al*., 2011). A piece of R10 rutile fragment separated from a large single crystal was used in this study. TIMS analyses for this rutile yield relatively high U concentration (*ca*. 50 ppm) and rather constant U–Pb age ranging from 1086.3 to 1096.6 Ma (^{206}Pb/^{238}U age) and from 1085.1 to 1096.2 Ma (^{207}Pb/^{235}U age) (Luvizotto *et al*., 2009). The 23 U–Pb spot analyses for this rutile obtained in this study are shown on the Concordia diagram (Fig. 2a), yielding a Concordia age of 1091.5 ± 9.6 Ma (2σ, decay constant errors included, MSWD = 0.21, Fig. 2a), which is vary consistent with the TIMS results. The weighted mean ^{206}Pb/^{238}U age is 1093 ± 10 Ma (95% confidence, MSWD = 0.33, Fig. 3a) and the weighted mean ^{207}Pb/^{235}U age is 1090 ± 10 Ma (95% confidence, MSWD = 0.14, Fig. 3b). Both ages are within the range of the reported TIMS ages.

Rutile standard DXK

This studied rutile comes from a rutile deposit located in Henshan Mountain of the Trans-North China Orogen, which has been described by Shi *et al*. (2012). It is one of the largest rutile deposits in China, with a resource of 6 million metric tons of titanium. Rutiles are hosted mainly by anthophyllite gneisses and mostly occur as euhedral tetragonal crystals or fragments with lengths ranging from 0.02 to 0.50 mm. They are mostly translucent and dark

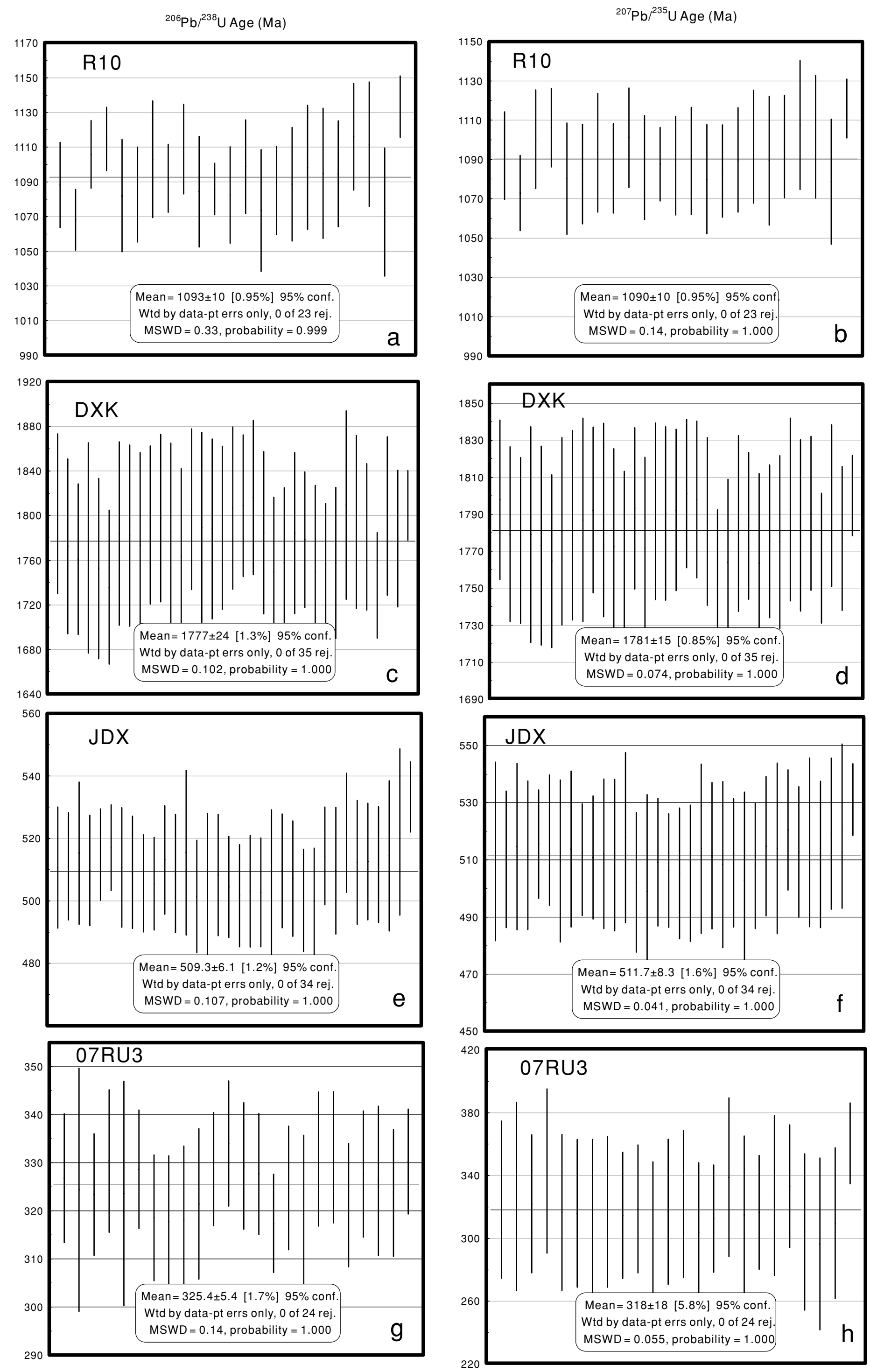

Fig. 3. Corrected ratios of $^{206}Pb/^{238}U$ and $^{207}Pb/^{235}U$ for standard rutiles R10 (a, b), DKX (c, d), JDX (e, f) and unknown sample 07RU3 (g, h). Data-point error bars are 1σ.

red to dark brown. Thirty rutile grains or fragments have been analyzed previously by Shi *et al*. using the SIMS method (sample RZ-1) (Shi *et al*., 2012). Their results indicate different rutile grains from this sample have relatively consistent and high U concentrations (~20 ppm) and almost identical U–Pb isotopic compositions, thus it is suitable to be used as an in house standard for quality control of *in situ* U–Pb rutile dating studies. The weighted mean SIMS $^{207}Pb/^{235}U$ age is 1779 ± 13 Ma (95% confidence, MSWD = 0.73) and the weighted mean of SIMS $^{206}Pb/^{238}U$ age is 1775 ± 23 Ma (95% confidence, MSWD = 0.75) (Shi *et al*., 2012). Thirty five rutile grains analyzed in this study comes from the same sample (RZ-1) analyzed by Shi *et al*. (2012). Our analytical results for this sample gave a Concordia age of 1781 ± 15 Ma (2σ, decay constant errors included, MSWD = 0.17, Fig. 2b) with a weighted mean $^{206}Pb/^{238}U$ age of 1777 ± 24 Ma (95% confidence, MSWD = 0.102, Fig. 3c) and a weighted mean $^{207}Pb/^{235}U$ age of 1781 ± 15 Ma (95% confidence, MSWD = 0.074). These results are very similar to the SIMS results.

Rutile standard JDX

Rutile JDX is a large gem-grade euhedral crystal, which is 5 cm in length and 2.5 cm in thickness. This rutile has been used as an in-house standard for SIMS analyses by the Institute of Geology and Geophysics, Chinese Academy of Sciences, Beijing (Li *et al*., 2011). Previous SIMS analyses on this rutile show that it contains 5–10 ppm of U and yields a weighted mean $^{207}Pb/^{235}U$ age of 513 ± 9 Ma and a weighted mean $^{206}Pb/^{238}U$ age of 509 ± 8 Ma (Li *et al*., 2011). In this study thirty four spots were analyzed on eight small fragments (~300 × 300 × 200 μm) in one mount. The U–Pb data cluster together on the Concordia diagram with a Concordia age 509.7 ± 6.2 Ma (2σ, decay constant errors included, MSWD = 0.37, Fig. 2c) and yield a weighted mean $^{206}Pb/^{238}U$ age of 509.3 ± 6.1 Ma (95% confidence, MSWD = 0.107, Fig. 3e) and a weighted mean $^{207}Pb/^{235}U$ age of 511.7 ± 8.3 Ma (95% confidence, MSWD = 0.041, Fig. 3f), which are within the error of the SIMS age.

Rutile sample 07RU3

The sample 07RU3 was collected from the eclogite block along the Akyazhi River, southwestern Chinese Tianshan. It is a rutile-bearing vein and the rutiles are centimeter-sized oriented acicular. Previous SIMS results for a single large crystal (~5 cm in diameter) from this sample indicated it has relatively uniform U content of 1.5 ± 0.3 ppm (1SD) (Li *et al*., 2011). Applying a ^{207}Pb based common lead correction method yields a weighted mean $^{206}Pb/^{238}U$ age of 320 ± 10 Ma (95% confidence, MSWD = 2.0, SIMS method) (Li *et al*., 2011). Twenty four rutile grains from the same mount were analyzed in this study. The U–Pb data are displayed on the Concordia diagram (Fig. 2d), which yields a Concordia age of 325.2 ± 5.6 Ma (2σ, decay constant errors included, MSWD = 0.56, Fig. 2d). These data give a weighted mean $^{206}Pb/^{238}U$ age of 325.4 ± 5.4 (95% confidence, MSWD = 0.14, Fig. 3g) and $^{207}Pb/^{235}U$ age of 318 ± 18 (95% confidence, MSWD = 0.055, Fig. 3h), consistent with the previous SIMS results.

Conclusions

This paper reports a new rutile U–Pb dating protocol using a MC-ICPMS coupled with an excimer 193 nm laser ablation system and its successful application to three reference rutile standards (R10, JDX and DXK) and one rutile sample (07RU3). The analytical results obtained by this protocol agree well with literature values or previous results, thereby demonstrating that this technique can yield precise and accurate U–Pb dating results for Paleozoic to Paleoproterozoic rutile even with ~1 ppm U.

Acknowledgments—Drs. Thomas Zack and Qiu-li Li are thanked for providing the tested rutile samples and standards. Dr. David Chew and another anonymous reviewer are thanked for their constructive comments and careful revision. This study was jointly supported by research grants from NSFC (No. 41173007) and the Chinese Academy of Sciences (GIGCAS-135-Y234151001) to Dr. X.-P. Xia. This is a contribution IS-1717 to the Guangzhou Institute of Geochemistry, the Chinese Academy of Sciences.

References

Birch, W. D., Barron, L. M., Magee, C. and Sutherland, F. L. (2007) Gold- and diamond-bearing White Hills Gravel, St Arnaud district, Victoria: age and provenance based on U–Pb dating of zircon and rutile. *Australian J. Earth Sci.* **54**, 609–628.

Bracciali, L. P., Randall, R., Horstwood, M. S. A., Condon, D. and Najman, Y. (2013) U–Pb LA-(MC)-ICP-MS dating of rutile: New reference materials and applications to sedimentary provenance. *Chem. Geol.*, doi:10.1016/j.chemgeo.2013.03.013.

Horn, I., Rudnick, R. L. and McDonough, W. F. (2000) Precise elemental and isotope ratio determination by simultaneous solution nebulization and laser ablation-ICP-MS: application to U–Pb geochronology. *Chem. Geol.* **164**, 281–301.

Horstwood, M. S. A., Foster, G. L., Parrish, R. R., Noble, S. R. and Nowell, G. M. (2003) Common-Pb corrected *in situ* U–Pb accessory mineral geochronology by LA-MC-ICP-MS. *J. Anal. Atom. Spectrom.* **18**, 837–846.

Kooijman, E., Mezger, K. and Berndt, J. (2010) Constraints on the U–Pb systematics of metamorphic rutile from *in situ* LA-ICP-MS analysis. *Earth Planet. Sci. Lett.* **293**, 321–330.

Kylander-Clark, A. R. C., Hacker, B. R. and Mattinson, J. M. (2008) Slow exhumation of UHP terranes: Titanite and rutile ages of the Western Gneiss Region, Norway. *Earth Planet. Sci. Lett.* **272**, 531–540.

Li, Q.-l., Lin, W., Su, W., Li, X.-h., Shi, Y.-h., Liu, Y. and Tang, G.-q. (2011) SIMS U–Pb rutile age of low-temperature eclogites from southwestern Chinese Tianshan, NW China. *Lithos* **122**, 76–86.

Luvizotto, G. L., Zack, T., Meyer, H. P., Ludwig, T., Triebold, S., Kronz, A., Munker, C., Stockli, D. F., Prowatke, S., Klemme, S., Jacob, D. E. and von Eynatten, H. (2009) Rutile crystals as potential trace element and isotope mineral stand-

ards for microanalysis. *Chem. Geol.* **261**, 346–369.
Morton, A. C. and Hallsworth, C. (1994) Identifying provenance-specific features of detrital heavy mineral assemblages in sandstones. *Sed. Geol.* **90**, 241–256.
Müller, W., Shelley, M., Miller, P. and Broude, S. (2009) Initial performance metrics of a new custom-designed ArF excimer LA-ICPMS system coupled to a two-volume laser-ablation cell. *J. Anal. Atom. Spectrom.* **24**, 209–214.
Pearce, N. J. G., Perkins, W. T., Westgate, J. A., Gorton, M. P., Jackson, S. E., Neal, C. R. and Chenery, S. P. (1997) A compilation of new and published major and trace element data for NIST SRM 610 and NIST SRM 612 glass reference materials. *Geostand. Newsl.* **21**, 115–144.
Shi, G., Li, X., Li, Q., Chen, Z., Deng, J., Liu, Y., Kang, Z., Pang, E., Xu, Y. and Jia, X. (2012) Ion microprobe U–Pb age and Zr-in-rutile thermometry of rutiles from the daixian rutile deposit in the Hengshan Mountains, Shanxi Province, China. *Econ. Geol.* **107**, 525–535.
Simonetti, A., Heaman, L. M. and Chacko, T. (2008) Use of discrete-dynode secondary electron multipliers with Faradays—A 'reduced volume' approach for *in-situ* U–Pb dating of accessory minerals within petrographic thin section by LA-MC-ICP-MS. *Laser Ablation ICP-MS in the Earth Sciences: Current Practices and Outstanding Issues: Mineralogical Association of Canada Short Course Series* (Sylvester, P., ed.), 241–264, Vancouver.
Stacey, J. S. and Kramers, J. D. (1975) Approximation of terrestrial lead isotope evolution by a two-stage model. *Earth Planet. Sci. Lett.* **26**, 25.
Storey, C. D., Smith, M. P. and Jeffries, T. E. (2007) *In situ* LA-ICP-MS U–Pb dating of metavolcanics of Norrbotten, Sweden: Records of extended geological histories in complex titanite grains. *Chem. Geol.* **240**, 163–181.
Vry, J. K. and Baker, J. A. (2006) LA-MC-ICPMS Pb–Pb dating of rutile from slowly cooled granulites: Confirmation of the high closure temperature for Pb diffusion in rutile. *Geochim. Cosmochim. Acta* **70**, 1807–1820.
Warren, C. J., Grujic, D., Cottle, J. M. and Rogers, N. W. (2012) Constraining cooling histories: rutile and titanite chronology and diffusion modelling in NW Bhutan. *J. Metamorphic Geol.* **30**(2) 113–130.
Xia, X., Sun, M., Zhao, G., Li, H. and Zhou, M. (2004) Spot zircon U–Pb isotope analysis by ICP-MS coupled with a frequency quintupled (213 nm) Nd-YAG laser system. *Geochem. J.* **38**, 191–200.
Xiao, Y., Sun, W., Hoefs, J., Simon, K., Zhang, Z., Li, S. and Hofmann, A. W. (2006) Making continental crust through slab melting: Constraints from niobium–tantalum fractionation in UHP metamorphic rutile. *Geochim. Cosmochim. Acta* **70**, 4770–4782.
Zack, T., Stockli, D. F., Luvizotto, G. L., Barth, M. G., Belousova, E., Wolfe, M. R. and Hinton, R. W. (2011) *In situ* U–Pb rutile dating by LA-ICP-MS: Pb-208 correction and prospects for geological applications. *Contrib. Mineral. Petrol.* **162**, 515–530.